

# A Catalog of Moving Group Candidates in The Solar Neighborhood

Jingkun Zhao, Gang Zhao, Yuqin Chen

## ABSTRACT

Based on kernel estimator and wavelet technique, we have identified 22 moving group candidates in the solar neighborhood from a sample which includes around 14000 dwarfs and 6000 giants. Six of them were previously known as the Hercules stream, the Sirius-UMa stream, the Hyades stream, the Caster group, the Pleiades stream and the IC 2391; five of them have also been reported by other authors. Eleven moving group candidates, not previously reported in the literature, show prominent structures in dwarf or giant samples. A catalog of moving group candidates in the solar neighborhood is presented in this work.

*Subject headings:* (Galaxy:) solar neighborhood-stars: kinematics-stars: abundance

## 1. Introduction

Since the first discovery of the two clearest examples of moving groups in the solar neighborhood (the Hyades and the Ursa) by Proctor (1869), the studies of moving group have been paid attention for a long time. There are two main techniques to detect moving groups. One is the convergent point (Brown 1950, Jones 1971) technique for proper motion data; the other is searching kinematic structure in velocity space. Most works adopted the second technique. For example, *Gómez et al.* (1990) used the SEM algorithm to decompose the sample into the sum of tridimensional gaussians in the (U,V,W) velocity, and concluded that the observed distribution of the residual velocity can be explained as the sum of four independent distributions which were related to several open clusters in the solar neighborhood. *Chen et al.* (1997) developed an algorithm using a non-parametric kernel estimator to describe the the stellar distribution in a 4-dimensional space ( velocities and age) and four moving groups near the Sun (Pleiades, Sirius, Hyades, IC2391) have been identified without

---

National Astronomical Observatories, Chinese Academy of Sciences, Beijing, 100012, China; gzhao@bao.ac.cn.

assuming any prior knowledge of moving groups, neither the velocity distribution nor other physical properties.

After the release of the Hipparcos Catalogue (ESA 1997), the research of moving groups in the solar neighborhood has made great progress since accurate parallaxes and proper motions for a large number of stars are available. (Skuljan et al. 1999) use the wavelet transform technique to analyze the distribution derived by an adaptive kernel method and also find several moving groups. Recent works by Famaey et al. (2005, 2007) have identified five moving groups based on 6000 giants and investigated the mass distribution of the Hyades stream based on the Geneva-Copenhagen survey of 14000 dwarfs from Nordström et al. (2004). Klement et al. (2008) identified at least four ‘phase space overdensities’ of stars on very similar orbits in the solar neighborhood using the 1<sup>st</sup> RAVE public data release. Different authors use different techniques and different samples, but they all report the presence of moving groups in the solar neighborhood.

With the newly-developed wavelet transform technique by Skuljan et al. (1999), we attempt to identify the stellar moving groups in the solar neighborhood by combining both the dwarf samples from Nordström et al. (2004) and the giant samples from Famaey et al. (2005). The main goals are to investigate whether the locations in velocity space of those groups derived from different samples are consistent as well as finding new streams based on large samples of stars and new method.

## 2. The method to identify moving group

Since the sample is in the solar neighborhood, the position of the stars does not provide any discriminant information for the detection of moving groups, so the detection in our paper mainly depends on the two components of the stellar velocity—the U component pointing towards the galactic, V component towards the direction of the galactic rotation. First, the probability density function  $f(U,V)$  is estimate by a kernel function, and next the wavelet transform will be carried out, so we can finally recognize the moving groups on the basis of the analysis of wavelet coefficients.

### 2.1. Density distribution

We use the kernel function to decide the probability density at any given point. The type of kernel function used in our method is a radial basis function (Equation 1).  $h$  is a smoothing parameter,  $(\Sigma)$  is the covariance matrix. The probability density of the  $(U,V)$

panel is then derived by Equation 2.  $n$  is the number of stars in our sample.

$$K(x, x_i) = \exp\left(-\frac{1}{2h^2}(x - x_i)^T(\Sigma)^{-1}(x - x_i)\right) \quad h > 0 \quad (1)$$

$$\rho(x) = \frac{1}{nh^2 2\pi |\Sigma|^{1/2}} \sum_{i=1}^n K(x, x_i) \quad (2)$$

## 2.2. Wavelet transform

After deriving the density of any given (U,V) point, in order to achieve the (U,V) center and the dispersion of the possible moving groups, we use two-dimension wavelet transform technique to analyze them (Skuljan et al. 1999). Wavelet analysis (Daubechies 1988; Chui 1992; Ruskai et al. 1992) is a fantastic tool and is becoming more and more popular in astronomical researches.

The wavelet transform provides an easily interpretable visual representation of  $\rho(x)$ . Moreover the continuous wavelet transform can be used in singularity detection. In this paper, we use it to find some structures working at different scales.

To process a wavelet transform of a function  $f(x,y)$ , we must define an analyzing wavelet  $\psi(x/\sigma, y/\sigma)$  called mother wavelet in advance.  $\sigma$  is scale variable. The wavelet coefficient of the point  $(\mu, \nu)$  then can be derived by Equation 3.

$$\omega(\mu, \nu) = \int_{-\infty}^{\infty} \int_{-\infty}^{\infty} f(x, y) \psi\left(\frac{x - \mu}{\sigma}, \frac{y - \nu}{\sigma}\right) dx dy \quad (3)$$

The actual choice of the analyzing wavelet  $\psi$  depends on the particular application. A mother wavelet named Mexican hat (Skuljan et al. 1999) is the second derivative of a Gaussian and generally gets good results when applied to find singularities. So when we intend to search for certain groups from a given data distribution, a two-dimensional Mexican hat is selected as the mother wavelet (Equation 4).

$$\psi(x, y, a) = \left(2 - \frac{x^2 + y^2}{a^2}\right) e^{-(x^2 + y^2)/2a^2} \quad (4)$$

The main characteristic of the function  $\psi$  is that the total volume is equal to zero, which is what enables us to detect any over-densities in our data distribution. The wavelet coefficients will be all zero if the analyzed distribution is uniform; but if there is any significant ‘bump’ in the distribution, the wavelet transform will give a positive value at that point.

### 3. Results and Discussions

Two data sets are selected as our samples. One is the 14000 dwarf (Nordström et al. 2004, hereafter Nord04 ); the other is 5311 K and 719 M giant (Famaey et al. 2005). The information of dwarf samples came from the Geneva-Copenhagen survey, in which the ages, metallicities and kinematic properties are provided, while that of the giant sample was obtained from CORAVEL/Hipparcos/Tycho-2. First the probability density was derived by the method (Sec 2.1). For equation 1, the smoothing parameter  $h$  should be carefully selected because small values of  $h$  emphasize noisy structure while large  $h$  value will smooth out all the details of the distribution. Our selection of the value  $h$  adopts the method of Asiain et al (1999). The value of  $h$  is set to be 0.145 for the dwarf sample and 0.117 for the giant sample. The density distribution in the (U,V) plane has some irregularities and can not be described by a unique velocity ellipsoid, and some ‘bumps’ can be clearly recognized. Famaey et al.(2008)derived the threshold of noise wavelet coefficients to have a value of  $10^{-4}$ . Thus, the coefficients smaller than  $10^{-4}$  in the present work will be rejected. Fig.1 shows the contour map of the positive wavelet coefficients obtained in the (U,V) space from  $a = 4\text{km}s^{-1}$ .

#### 3.1. Monte Carlo simulation

After obtaining the probability density of the samples and the wavelet coefficient contour map, the results show several features. However, are these features real or are they caused by some noise? There are several factors that will affect the observed number of stars in each bin: such as the measurement error, statistical fluctuations related to the finite sample, etc. We can expect that the number of the observed stars in each bin will subject Poisson distribution with an average of  $\bar{N}$  which can be derived by the probability density function multiplied with factor  $nS$ , where  $n$  is the total number of stars and  $S$  is area covered by a square bin. To investigate how probable are the features showed in Fig.1, we generate a large number ( $N=2000$ ) of Poisson random copies. For each copy, we get a wavelet positive coefficient map (after rejecting those smaller than  $10^{-4}$ ). Fig.2 is a example of one copy. The probability of those features is shown in Table 1. Typically, only those features with 90 percent or better probability are considered to be real.

### 3.2. The detected moving groups

From Fig.1, it is clear that stars are clumped at different locations in the (U,V) space. Table 1 shows the central (U,V) of 22 possible moving groups detected by either the dwarf sample or the giant sample by using the wavelet technique. We analyzed the dwarf sample and the giant star sample separately because the star numbers in the solar neighborhood of dwarf and giant stars are different due to different lifetimes with more dwarf stars than giant stars. In view of this, merging the two types of stars into one sample will reduce the statistically grouped structure in the (U,V) space. In some cases, the giant sample can give better structure than the dwarf sample as we will show later (for group 7). It seems that a more reasonable way is the comparison of these grouped structures detected from both the dwarf and giant sample and check if they can give consistent results. In this sense, we have found that the central (U,V) values of these groups between the two samples are quite consistent from 12 groups.

Among these groups, groups 1 to 5 are quite strong and they have been widely reported to be moving groups in the literature. As we can compare our results with previous works by Eggen (1991, 1992a, b, c) based on the FK5 catalogue and Dehnen (1998), we found good agreement for the Pleiades (group 1), Hyades (group 2) and Sirius (group 4). Specifically, our values are quite consistent with those of Dehnen (1998), who gave mean motions of (-12, -22), (-40, -20.0), (9, 3),  $\text{kms}^{-1}$  for the Pleiades, Hyades and Sirius groups, respectively, based on the sample of 14369 stars observed by the Hipparcos satellite. Eggen (1991, 1992a, b, c) showed mean motions of (-11.6, -20.7), (-40.0, -17.0), (14.9, 1.3)  $\text{kms}^{-1}$  for the Pleiades, Hyades and Sirius are somewhat updated by using Hipparcos parallaxes. Our values are also similar to those values in recent works by Famaey et al. (2007) and Antoja et al (2008). Mean motions of group 3 is also in agreement with the Hercules stream centered at (-35, -45) found by Fux (2001). It is noticed that the mean motions of group 3 are slightly different between the dwarf and giant groups. Considering that the giant group shows better structure than that of the dwarf group in Fig. 1, we suggested that the mean motions of giant groups have more reasonable values for group 3. Our group 5 with mean motions of (-11, -7) in the present work is very similar to the Castor group with (-10, -10), which is classified as a young group by Famaey et al. (2007) with mean motion of (-10, -12).

Besides the five known moving groups, two moving groups (group 6 and group 7) with mean motions of (38, -20) and (-57, -45) are quite significant from both dwarf and giant samples and the probability from our simulation is larger than 98%. For our Group 6, Antoja et al. (2008) also suggest the structure centered at (35, -20) to be a new group. However, since the structure is weak in their work, they considered it as part of the elongation of the Sirius or Coma Berenices structure. However, Group 6 is very prominent and has a well-

defined shape in the present work both for the dwarf sample and giant sample. Moreover, their mean motions are far away from those of Sirius and the Coma Berenices structures without significant connections in the contour plot of Fig. 1. Note that the giant sample of group 6 has some extension to the south-west direction, which disappears in the simulation contour of Fig.2 after adding noise while the center part of group 6 persists. It seems that the center part of group 6 is real while the extension to the south-west direction may be noise. In this sense, we suggest that group 6 is real in the giant sample, and it is very significant in dwarf sample.

The other five groups (8, 9, 10, 12, 14) also have some features in both the dwarf sample and the giant sample and the simulation shows that four of them are significant with probability above 90% of being real, except for the group 10 with the probabilities of 86% and 82%. The rest of the groups are shown only in the dwarf sample (15 and 16) or only in the giant sample (11, 13, 17, 18, 19, 20, 21, 22); but four groups (11, 13, 17, 21) are not very significant with the probability lower than 90% by simulation. Interestingly, some of these features have been reported by previous works. For example, our group 14 is consistent with the IC 2391 stream, which shows a mean motion of (-20.8, -15.9) by Eggen (1992b) and of (U=-20, V=-12) by Chen et al.(1997). Moreover, our groups 18, 20 and 22 may be the same groups as No. 7, 14 and 13 in Table 3 of Antoja et al (2008), which summarizes the possible grouping structures from Dehnen(1998) and Eggen’s serial papers.

A catalog of 22 possible moving group candidates are listed in Table 1, although some of them are not so significant (10, 11, 13, 17, 21) for a statistical requirement of the probability above 90%. Certainly, these groups with low probabilities from our statistical analysis need further study. The metallicity is only available in the dwarf sample, based on which we present the peak and scatter of [Fe/H] for all the candidates in Table 1.

### 3.3. The W velocity distributions of the groups

Although all the works to detect the moving groups do not take into account the W velocity, this component may bring some new information. Therefore, we have generated the (V,W) and (U,W) contour plots with the same method. As expected, the distribution of W velocity is limited to a narrow range from -20 km/s to 5 km/s for both the dwarf and giant samples. Moreover, the dispersion in the W velocity for these groups is about 10-15 km/s, which is significantly larger than those of the U and V components of 4-6 km/s in defining these groups. Thus, the (V,W) and (U,W) contour plots have no advantages in identifying possible moving groups. Several groups of the 22 candidates actually belong to the same groups in the (V,W) and (U,W) contour plots. Note that the groups of 9 and 12

have the largest  $W$  dispersion of 20 km/s because they have very weak features in our Fig.1. In general, these moving group candidates based on the  $(U,V)$  contour are considered to be more reliable by taking into account the large scatter in the  $W$  component distribution.

Our Group 3 and Group 7 appear to coincide with the Hercules group identified as green lumps in Fig.1 of Famaey et al 2008 and they think the green lumps are both the Hercules group. However, the argument is not significant and we suggest that they may be distinct group. Fig.3 shows the statistical result of the  $Z_{\max}$  distribution with the cut of  $Z_{\max} < 1.0$  kpc. It seems that the peak of Group 3 in the  $Z_{\max}$  distribution is at 0.1-0.2 kpc while there is a large contribution from stars with  $Z_{\max}$  of 0.2-0.3 kpc for Group7. Moreover, from Famaey et al (2004), it is clear that the  $\sigma(U, V, W)$  of the Hercules group is significantly higher than those of the Hyades or Sirius, which could indicate an overlapping of more than one distinct group. In the present work, the  $\sigma(U, V, W)$  is nearly the same for group 3 and group7 as well as other groups. Finally, there is also a hint of  $[\text{Fe}/\text{H}]$  deviation with the average  $[\text{Fe}/\text{H}]$  of -0.16 dex in group 3 versus -0.22 dex for group 7. Further study on this topic is necessary before firm conclusions can be drawn.

#### 4. Conclusions

Using the dwarfs and giants in the solar neighborhood, we illustrate a detailed analysis of the UV distribution. This analysis reveals 22 possible grouping structures identified by the kernel estimator and wavelet technique. The location in velocity space of 12 possible moving groups from both dwarf and giant samples are consistent. 11 groups, including the five well-known groups, Pleiades, Hyades, Hercules, Sirius and Castor streams, are consistent with previous works. Eight groups, not reported by previous works, are presented and most of them are thought to be significant in term of statistics. In summary, a catalog of 22 moving group candidates with the centers  $(U,V,W)$ , their dispersions and mean metallicity are given.

This study is supported by the National Natural Science Foundation of China under grants No. 10521001, 10673015, 10433010, the National Basic Research Program of China (973 program) No. 2007CB815103/815403 and by the Ministry of Science and technology of China under grant No. 2006AA01A120.

## REFERENCES

- Antoja T., Figueras F., Fernandez D., Torra J., 2008, ApJS, 179, 326
- Asiain R., Figueras F., Torra J., Chen B., 1999, A&A, 341, 427
- Brown, A., 1950, ApJ, 112, 225
- Chen B., Asiain R., Figueras F., Torra J. 1997, A&A, 318, 29
- Chui C. H., 1992, Wavelet Analysis and its Application (New York: Academic)
- Daubechies I., 1988, Pure Appl. Math. 41, 909
- Dehnen, W., 1998, AJ, 115, 2384
- Eggen O.J., 1971, PASP, 83, 251
- Eggen O.J., 1991, AJ, 102, 2028
- Eggen O.J., 1992a, AJ, 103, 1302
- Eggen O.J., 1992b, AJ, 104, 1482
- Eggen O.J., 1992c, AJ, 104, 1493
- Eggen O.J., 1983, AJ, 88, 642
- Eggen O.J., 1996, AJ, 112, 1595
- Famaey B., Jorissen A., Luri X., Mayor M., Udry S., Dejonghe H. and Turon C.,  
arxiv:0411540
- Famaey B., Jorissen A., Luri X., Mayor M., Udry S., Dejonghe H. and Turon C., 2005, A&A,  
430, 165
- Famaey B., Pont F., Luri X., Udry S., Mayor M., Jorissen A., 2007, A&A, 461, 957
- Famaey B., Siebert A., Jorissen A., 2008, A&A, 483, 453
- Fux R., 2001, A&A, 373, 511
- Girardi L., Bressan A., Bertelli G. and Chiosi C., A&AS, 141,
- Gomez A.E., Delhaye J., Grenier S., Jäschek C., Arenou F., Jäschek M., 1990, A&A, 236,95
- Grebel G. K., Roberts W. J., 1995, A&AS,



Jones, D. H. P., 1971, MNRAS, 152, 231

Klement R., Fuchs B., and Rix H. W., 2008,ApJ, 685, 261

Nordström B., Mayor M., Andersen J., Holmberg J., Pont F., JØrgensen B. R., Olsen E. H.,  
Udry S. and Mowlavi N., 2004, A&A, 418, 989

Paulson D. B., Sneden C., Cochran W. D., 2003, AJ, 125, 3185

Proctor, R. A., 1869, Proceedings of the Royal Society of London, 18, 169

Ruskai M. B., Beylkin G., Coifman, R. Daubechies I., Mallat S., Meyer Y., Raphael L., 1992,  
Wavelets and Their Applications (Boston: Jones Bartlett)

Skuljan J., Hearnshaw J. B., Cottrell P. L., 1999, MNRAS, 308,731

Taylor B.J., 1999, AAS, 159, 100

Taylor B.J., & Honer M.D., 2005, ApJS, 159, 100

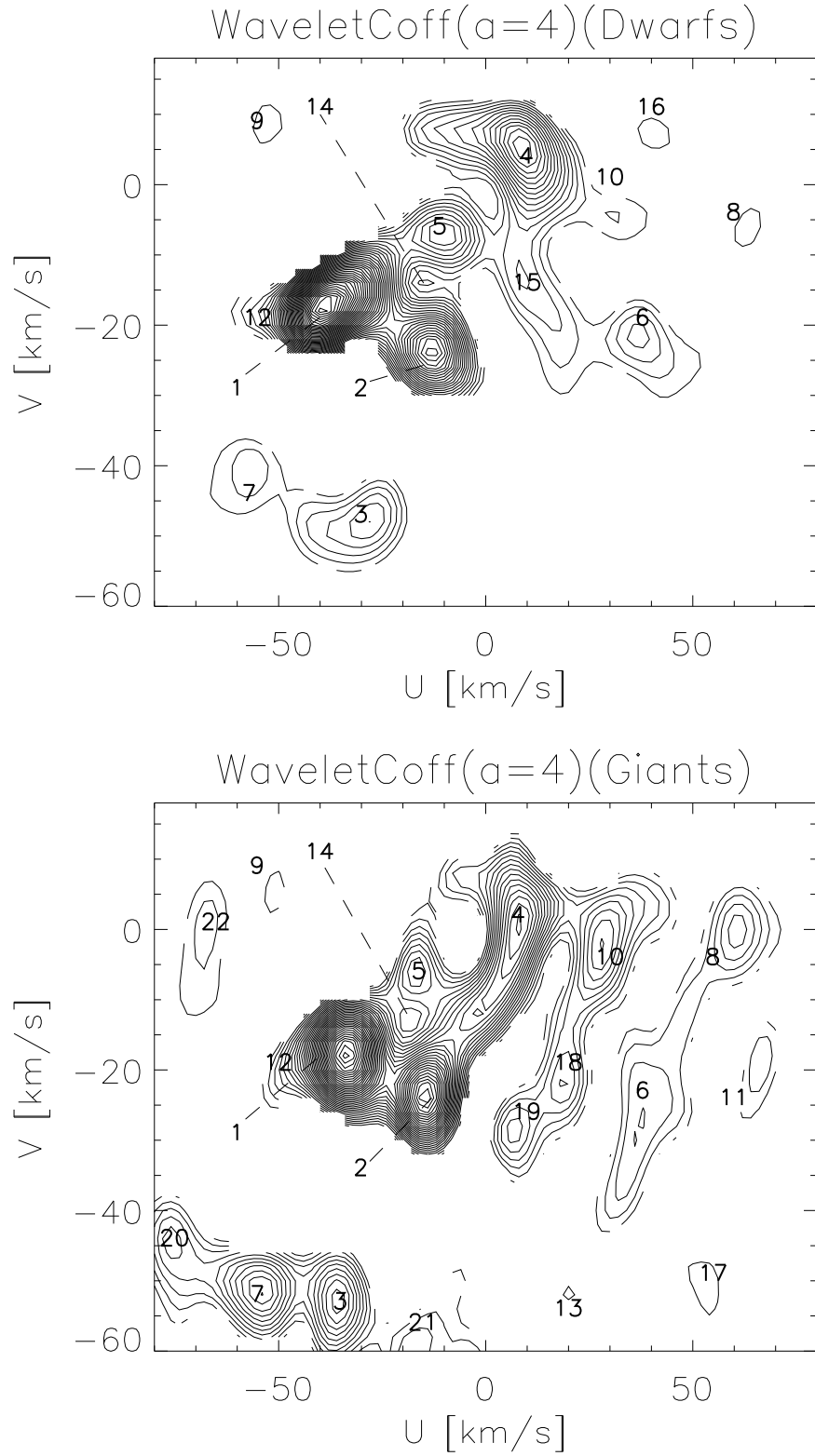


Fig. 1.— The contour map of the positive wavelet transform coefficient. The up is for dwarf sample and the bottom is for giant sample. The number is the sequence of the moving groups

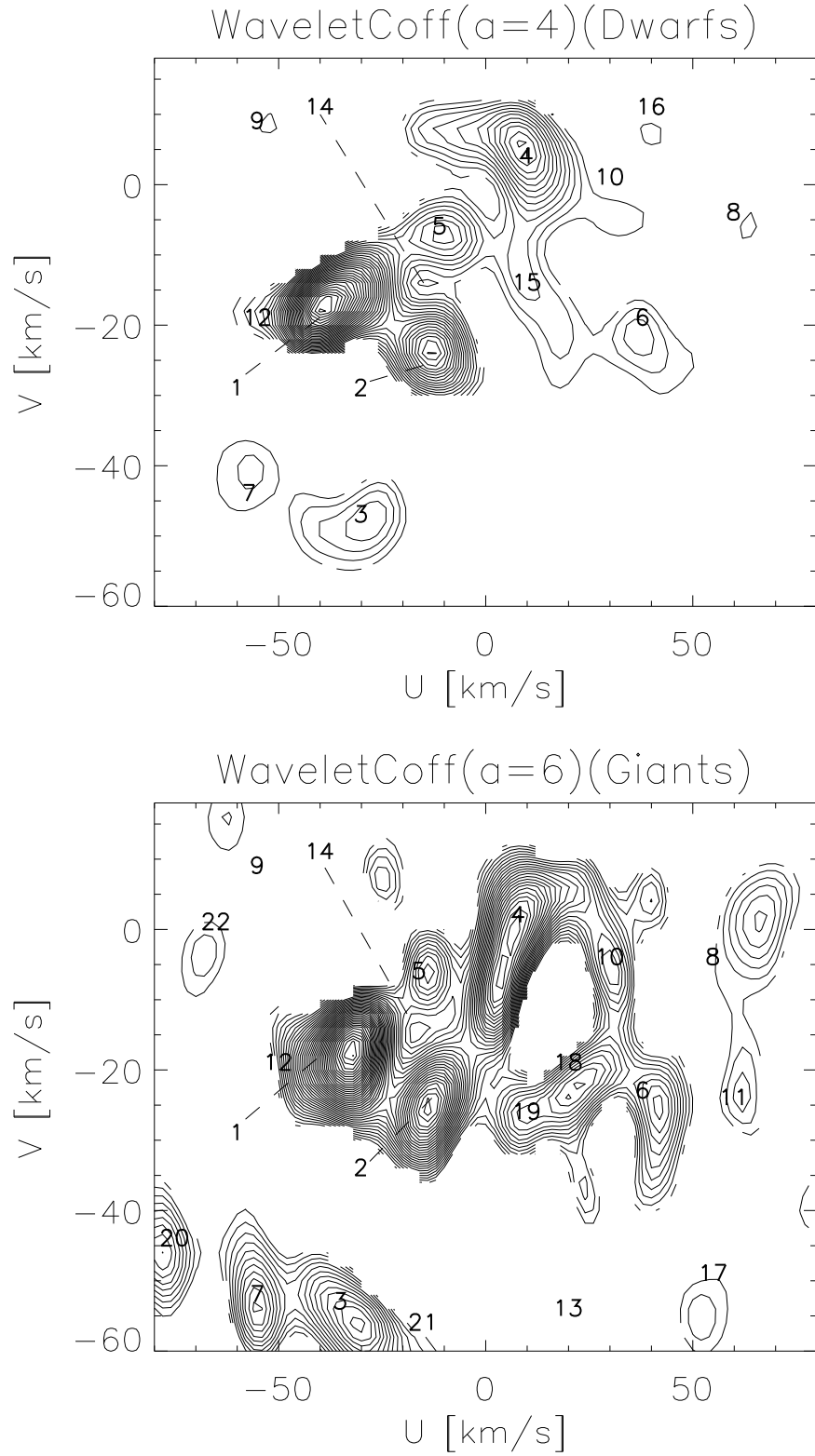


Fig. 2.— The contour map of positive wavelet transform coefficient for one copy of simulation

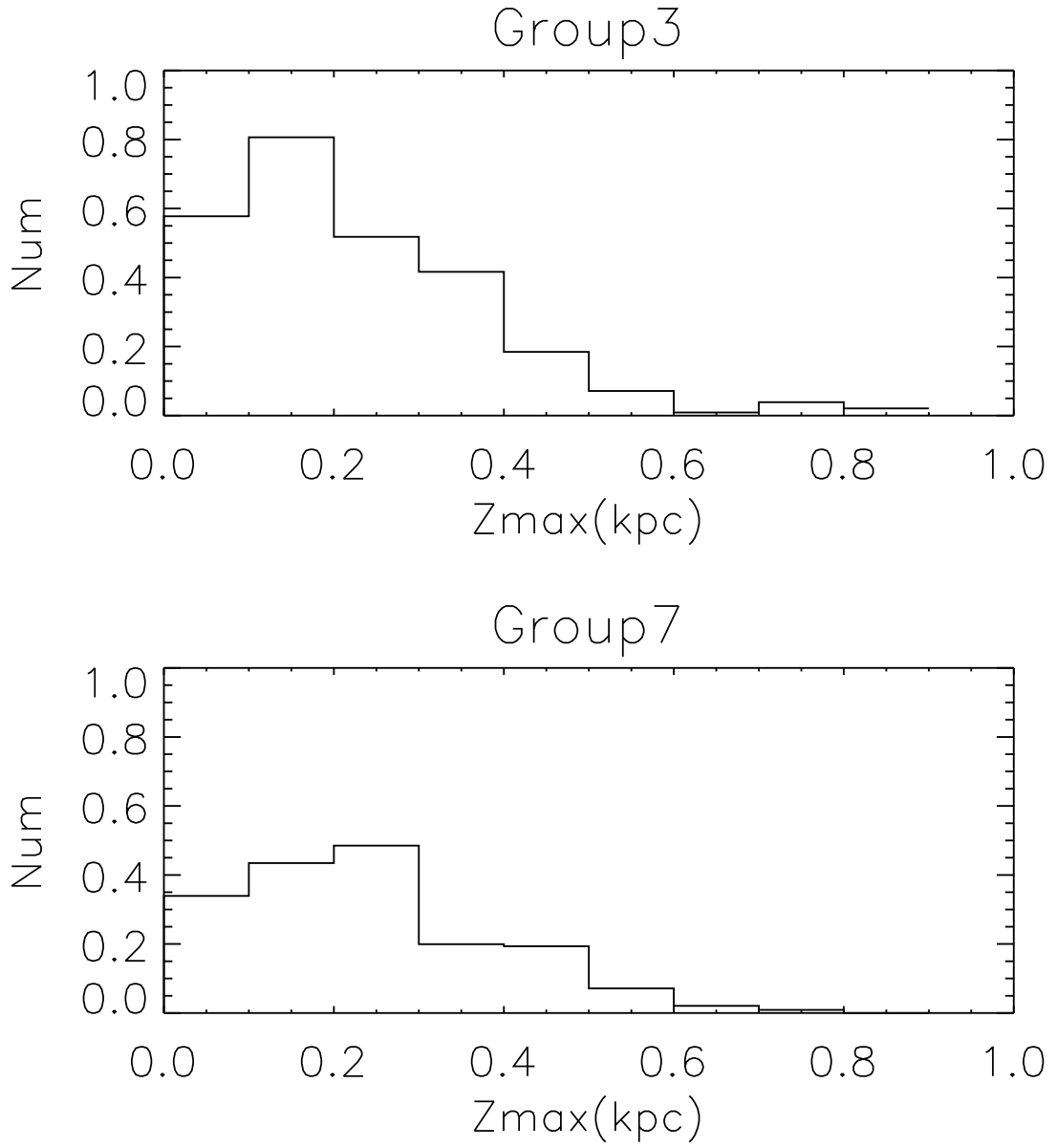


Fig. 3.— The  $Z_{\max}$  distributions of Group 3 and Group 7

Table 1. The heliocentric velocities of the moving groups detected by the dwarf sample and the giant sample. The column 1 is the sequence number of the groups. the column 2 and column 5 are the velocity center of the groups: column 2 is that detected by the dwarf sample; column 5 is that detected by the giant sample. Column 3 is the  $\sigma(U, V, W)$  for dwarfs and column 6 is that for giants. Column 4 is the detected probability of each moving group during the simulation for dwarf sample while column 7 is that for giant sample; column 8 is the average  $[\text{Fe}/\text{H}]$  of the groups; column 9 is the  $\sigma[\text{Fe}/\text{H}]$  of the groups; column 10 is the  $Z_{\text{max}}$  peak value of each group; the last column is the name of the corresponding moving group identified before(A08 is from Antoja et al 2008 and T3 means Table 3 in that paper; F08 is from Famaey et al 2008 and F.3 means Fig.3 in that paper)

No	Dw(U,V,W)	$\sigma_d(U, V, W)$	Dw(P)	Gi(U,V,W)	$\sigma_g(U, V, W)$	Gi(P)	$[\text{Fe}/\text{H}]$	$\sigma[\text{Fe}/\text{H}]$	$Z_{\text{max}}$	Moving Group
1	-38,-18,-10	6,6,10	100%	-38,-17,-11	6,6,12	100%	-0.09	0.17	0.1-0.2	Hyades
2	-12,-23,-10	6,6,10	100%	-15,-23,-10	6,6,12	100%	-0.17	0.17	0.1-0.2	Pleiades
3	-32,-48,-15	5,5,12	100%	-35,-51,-11	5,5,15	100%	-0.16	0.20	0.1-0.2	Hercules
4	10,3,-11	6,6,10	100%	10,3,-14	6,6,13	100%	-0.21	0.15	0.0-0.1	Sirius-UMa
5	-11,-7,-12	5,5,10	100%	-13,-6,-10	5,5,15	97%	-0.20	0.17	0.0-0.1	Coma(or Castor)
6	38,-20,-15	4,4,12	100%	37,-25,-12	4,4,14	98%	-0.24	0.21	0.1-0.2	A08(new feature)
7	-57,-45,-16	5,5,13	100%	-55,-50,-16	5,5,14	98%	-0.22	0.29	0.2-0.3	F08(F.3 green)
8	57,-5,-10	3,3,12	93%	60,-5,-10	5,5,18	87%	-0.28	0.18	0.2-0.3	
9	-56,7,1	3,3,21	97%	-50,4,3	3,3,20	90%	-0.28	0.17	0.1-0.2	
10	30,-5,-11	3,3,6	87%	28,0,-11	6,6,5	86%	-0.25	0.13	0.2-0.3	
11				65,-20,-7	5,8,16	63%			0.2-0.3	
12	-53,-19,-12	3,3,21	92%	-50,-20,-18	3,3,10	93%	-0.20	0.24	0.2-0.3	
13				20,-50,-5	3,3,22	82%			0.1-0.2	
14	-16,-15,-12	4,3,10	90%	-18,-15,-16	4,3,5	91%	-0.13	0.10	0.0-0.1	IC 2391
15	9,-15,-9	5,6,12	97%				-0.09	0.22	0.0-0.1	
16	42,8,-29	3,3,15	92%				-0.20	0.22	0.2-0.3	
17				55,-50,10	4,4,2	86%			0.2-0.3	
18				20,-20,-15	5,5,4	90%			0.1-0.2	A08(T3.No7)
19				8,-27,-8	5,5,13,2	93%			0.2-0.3	
20				-75,-46,-13	5,5,11	91%			0.1-0.2	A08(T3.No14)
21				-17,-49,-10	5,5,13	82%			0.2-0.3	
22				-69,-2,-10	5,5,22	90%			0.1-0.2	A08(T3.No13)

Table 2. The center velocity in literature corresponding groups in resent work. The column 1 is the sequence number of the groups in our work. Column 2 is from Dehnen(1998); Column 3 is from Eggen(1971, 1991, 1992a, b, c, 1996); column 4 is from Fux(2001); column 5 is from Famaey(2005); column 6 is according to Famaey(2007); column 7 is given by Famaey(2008); column 8 is from Klement(2008); column 9 is from Antoja (2008)

No	D(U,V)	E(U,V)	Fu(U,V)	F05(U,V)	F07(U,V)	F08(U,V)	K08(U,V)	A08(U,V)
1	-40,-20	-40.4,-16.0	-42,-18		-37,-17	-35,-18	-25,-15 <sup>a</sup>	Tab.3 No2
2	-12,-22	-11.6,-20.7	-13,-19		-15,-25	-16,-23	-25,-15 <sup>a</sup>	Tab.3 No1
3		-30.0,-50.0	-35,-45	-42,-51	-30,-50	-35,-51	-20,-50	Tab.3 No16
4	9,3	14.9,1.4	9,3	6.5,3.9	10,-5	5,1.5	6,4	Tab.3 No3
5	-10,-5		-3,-4		-10,-10			Tab.3 No4
6								35,-20
7						-55,-51		
8								
9								
10								
11								
12								
13	15,-60	5.8,-59.6						Tab.3 No6
14		-20.8,-15.9						Tab.3 No12
15								
16								
17								
18	20,-20							Tab.3 No7
19								
20	-70,-50							Tab.3 No14
21								
22	-70,-10							Tab.3 No13

<sup>a</sup>The group 1 and 2 were unresolved by Klement(2008).